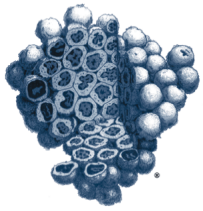

STEM CELLS®

Human Dental Pulp Stem Cells Improve Left Ventricular Function, Induce Angiogenesis, and Reduce Infarct Size in Rats with Acute Myocardial Infarction

Carolina Gandia, Ana Armiñan, Jose Manuel García-Verdugo, Elisa Lledó, Amparo Ruiz, M Dolores Miñana, Jorge Sanchez-Torrijos, Rafael Payá, Vicente Mirabet, Francisco Carbonell-Uberos, Mauro Llop, Jose Anastasio Montero and Pilar Sepúlveda

Stem Cells 2008;26;638-645; originally published online Dec 13, 2007;
DOI: 10.1634/stemcells.2007-0484

STEM CELLS®

TISSUE-SPECIFIC STEM CELLS

Human Dental Pulp Stem Cells Improve Left Ventricular Function, Induce Angiogenesis, and Reduce Infarct Size in Rats with Acute Myocardial Infarction

CAROLINA GANDIA,[a] ANA ARMIÑAN,[a] JOSE MANUEL GARCÍA-VERDUGO,[a,b] ELISA LLEDÓ,[a] AMPARO RUIZ,[b] M DOLORES MIÑANA,[c] JORGE SANCHEZ-TORRIJOS,[c] RAFAEL PAYÁ,[c] VICENTE MIRABET,[d] FRANCISCO CARBONELL-UBEROS,[d] MAURO LLOP,[a] JOSE ANASTASIO MONTERO,[a,e] PILAR SEPÚLVEDA[a,c]

[a]Unidad de Cardiorregeneración, Centro de Investigación Príncipe Felipe, Valencia, Spain; [b]Universidad de Valencia, Valencia, Spain; [c]Fundación Hospital General Universitario, Valencia, Spain; [d]Centro de Transfusion de la Comunidad Valenciana, Valencia, Spain; [e]Servicio de Cirugía Cardiaca, Hospital Universitario La Fe, Valencia, Spain

Key Words. Stem cell therapy • Ventricular remodeling • Left ventricular function • Dental pulp stem cells • Mesenchymal stem cells

ABSTRACT

Human dental pulp contains precursor cells termed dental pulp stem cells (DPSC) that show self-renewal and multilineage differentiation and also secrete multiple proangiogenic and antiapoptotic factors. To examine whether these cells could have therapeutic potential in the repair of myocardial infarction (MI), DPSC were infected with a retrovirus encoding the green fluorescent protein (GFP) and expanded ex vivo. Seven days after induction of myocardial infarction by coronary artery ligation, 1.5×10^6 GFP-DPSC were injected intramyocardially in nude rats. At 4 weeks, cell-treated animals showed an improvement in cardiac function, observed by percentage changes in anterior wall thickening left ventricular fractional area change, in parallel with a reduction in infarct size. No histologic evidence was seen of GFP^+ endothelial cells, smooth muscle cells, or cardiac muscle cells within the infarct. However, angiogenesis was increased relative to control-treated animals. Taken together, these data suggest that DPSC could provide a novel alternative cell population for cardiac repair, at least in the setting of acute MI. STEM CELLS *2008;26:638–645*

Disclosure of potential conflicts of interest is found at the end of this article.

INTRODUCTION

Mesenchymal stem cells (MSC) constitute a heterogeneous population found first in bone marrow (BM) and later in multiple tissues like adipose tissue, skin, cartilage, umbilical cord, placenta, and dental pulp [1–6]. Although MSC from multiple sources share multiple cell surface antigens, they show different pluripotency in vitro depending of their source of origin [7], which suggests that they could behave differently in vivo [8]. Several studies reported the therapeutic benefits of injection of bone marrow- or adipose-derived MSC after myocardial infarction (MI) and other heart diseases [9–12]. Transplantation of MSC resulted in improved ventricular function that was commonly associated with the induction of angiogenesis and myogenesis. To our knowledge, no studies have been performed to determine the therapeutic potential of dental pulp-derived MSC when they are transplanted after MI.

Dental pulp stem cells (DPSC) were first described as MSC-like odontogenic precursor cells with highly proliferative potential able to regenerate dentin in an immunocompromised host [6]. Although there are few reports comparing the antigenic features of DPSC and BM-MSC, cDNA microarray studies show that they differ in the expression of only a small number of genes [13, 14]. However, DPSC show higher self-renewal ability, immunomodulatory capacity, and proliferation in vitro than BM-MSC, and they differentiate preferentially to osteoblasts rather than to adipocytes [6, 15]. These cells, like BM-MSC, are able to secrete vascular endothelial growth factor (VEGF) [16–18], insulin-like growth factor-1 (IGF-1) and -2 (IGF-2) [13, 19, 20], stem cell factor (SCF), and granulocyte-colony stimulation factor [21, 22], all of which can exert proangiogenic, antiapoptotic, and cardioprotective actions [3, 23, 24]. Thus, the aim of this study was to determine whether DPSC could be useful for cardiac repair, in a rat model of MI.

MATERIALS AND METHODS

All procedures were approved by the Instituto de Salud Carlos III and institutional ethical and animal care committees.

Animals

A total of 50 male nude rats weighing 200–250 g (HIH-Foxn1 rnu; Charles River Laboratories, Wilmington, MA, http://www.criver.com) were included in the study. Seventeen died because of the surgical procedure during either induction of MI or cell transplantation. Animals with infarcts smaller than 25% of the left ventricular free wall after MI were excluded, which left 28 animals that were randomly divided in three experimental groups (saline, DPSC, and

Correspondence: Pilar Sepúlveda, Ph.D., Fundación Hospital General Universitario, Consorcio Hospital General Universitario de Valencia, Avenida Tres Cruces s/n, 46014 Valencia, Spain. Telephone: 34-961972146; Fax: 34-961972145; e-mail: pilar.sepulveda@uv.es, http://www.uv.es/sepulves Received June 19, 2007; accepted for publication December 4, 2007; first published online in STEM CELLS *EXPRESS* December 13, 2007. 1066-5099/2008/$30.00/0 doi: 10.1634/stemcells.2007-0484

BM-MSC) to perform all the assays. The survival rate in all groups was 100%.

Cells, Culture Conditions, and Retroviral Transduction of DPSC

BM-MSC were purchased from Inbiomed (San Sebastian, Spain, http://www.inbiomed.org) and expanded following the manufacturer's instructions. Human dental pulp ($n = 3$) was obtained from third molars, which were extracted for orthodontic reasons from healthy young people (18–21 years of age) who gave their informed consent. The teeth were immediately cracked open, and the pulp tissue was removed and processed. Pulp was minced into small fragments (<1 mm^3) prior to digestion in a solution of 2 mg/ml collagenase type I (Gibco, Grand Island, NY, http://www.invitrogen.com) for 90 minutes at 37°C. After centrifugation, cells were seeded in culture flasks with growth medium (Dulbecco's modified Eagle's medium with low glucose supplemented with 10% fetal calf serum [Invitrogen] and antibiotics) in a humidified atmosphere of 95% air and 5% CO_2 at 37°C. Nonadherent cells were removed 48 hours after the initial plating. The medium was replaced every 3 days. When primary culture became subconfluent, after 10–12 days, cells were collected by trypsinization and subcultured at 5,000 cells per cm^2 in growth medium. For enhanced green fluorescent protein (GFP) transduction, DPSC were seeded at 1,500 cells per cm^2. To label the cells, supernatants containing retroviral eGFP particles obtained from the PG13-PSF-green fluorescent protein (GFP) packaging cell line were filtered through a 0.45-μm filter, added to DPSC for 5 hours, and then replaced by fresh medium. This procedure was repeated daily for 3 days. Transduction efficiency was evaluated by flow cytometry. To assess the proliferative capacity of DPSC and GFP-DPSC, parallel cultures from three different donors were submitted to 12 serial passages. Population doublings (PD) were calculated using the formula PD = $[(\log_{10}(N_H) - \log_{10}(N_1)]/\log_{10}$ (2), where N_H is the cell harvest number and N_1 the inoculum cell number [7]. Cumulative population doublings were calculated, adding to each passage the PD of the previous passage. In vitro differentiation of DPSC to adipocytes or osteocytes was performed as previously described [15].

Flow Cytometry

Human DPSC (passages 3–10) were characterized by flow cytometry (EPICS XL flow cytometer; Beckman Coulter, Fullerton, CA, http://www.beckmancoulter.com) using anti-human monoclonal antibodies directly conjugated to fluorescein isothiocyanate (CD105 [AbD Serotec, Raleigh, NC, http://www.ab-direct.com], CD106 and CD44 [BD Pharmingen, San Diego, http://www.bdbiosciences.com/index_us.shtml], and CD14 and CD45 [Becton, Dickinson and Company, San Jose, CA, http://www.bd.com]) or phycoerythrin (CD117, CD34, CD166, CD29, CD90, and vascular endothelial growth factor receptor 2 [VEGFR-2] [Becton Dickinson]). Data acquisition and analyses were performed with Expo32 software (Beckman Coulter). The cells were labeled according to standard protocols. Matched labeled isotypes were used as controls.

Myocardial Infarction and Cell Transplantation

An animal model of myocardial infarction was conducted by ligation of the left coronary artery as previously described [25]. Rats were intubated and anesthetized (mixture of O_2/Sevorane [Abbott Laboratories, Madrid, Spain, http://www.Abbott.es]; rate, 100 cycles per minute; tidal volume, 2.5 ml; small animal ventilator model 683 [Harvard Apparatus, Holliston, MA, http://www.harvardapparatus.com]), and after thoracotomy, the acute MI was induced by permanent ligation of the left descending coronary artery with 6-0 Prolene (Braun, Barcelona, Spain, http://www.braun.com). The infarcted area was visualized after ligation by development of a pale color in the distal myocardium. The incision was closed with a 3-0 silk suture, and Nolotil (Ingelheim, Germany, http://www.boehringer-ingelheim.es) (0.4 g/ml) was given intraperitoneally (0.5 ml/kg) as a pain palliative. Transplantation was performed in the subacute phase of MI [26]. Briefly, 7 days later, rats were anesthetized and reopened by a midline sternotomy to perform intramyocardial transplantation (10^6 GFP-DPSC or an

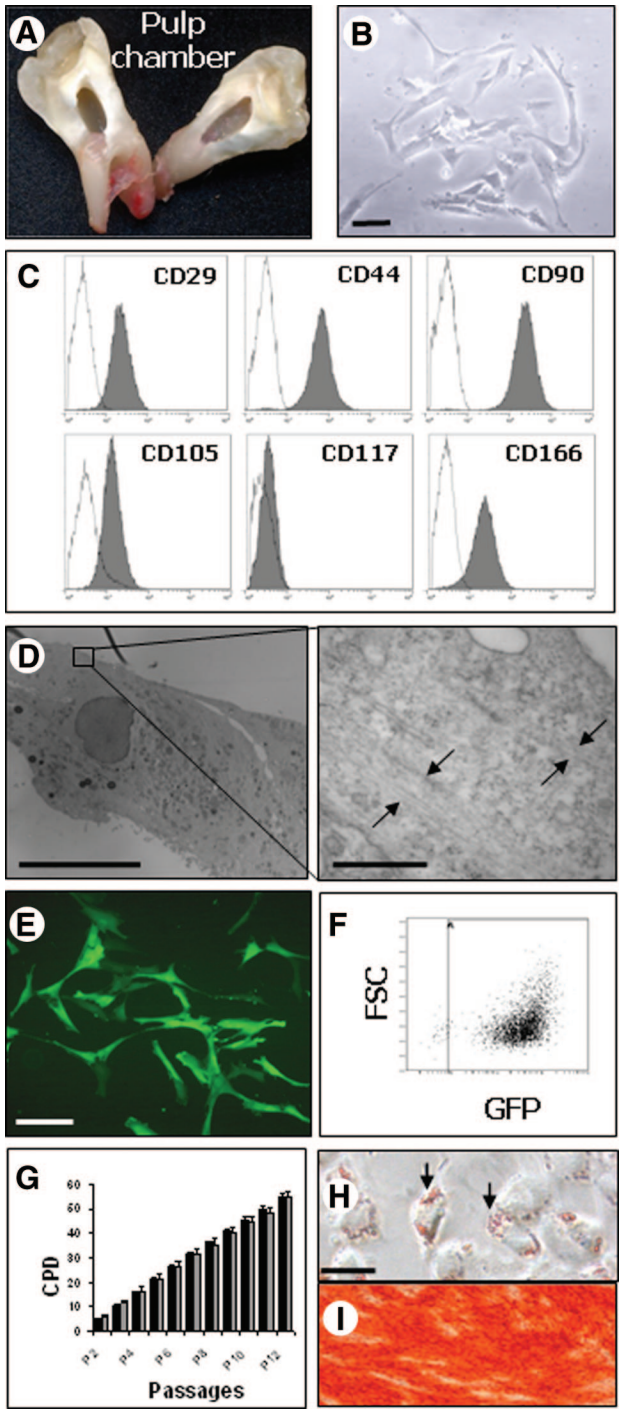

Figure 1. Characterization of primary human dental pulp stem cells (DPSC). **(A):** Cracked teeth showing the pulp chamber. **(B):** Cultured DPSC show a fibroblastic-like morphology. **(C):** A representative flow cytometric analysis of antigenic expression is shown. Shaded histograms represent staining with specific antibodies, and open histograms correspond to matched isotypes. **(D):** Ultrathin section of a DPSC in culture showing a detail of cytoplasmic ultrastructure. **(E):** Fluorescence photomicrograph of a GFP retrovirally labeled DPSC culture. **(F):** A representative flow cytometric analysis of GFP-DPSC. **(G):** Cumulative population doubling of DPSC (black columns) and GFP-DPSC (gray columns) from P2 to P12. **(H):** Adipogenic differentiation of GFP-DPSC. Arrows point to oil red O-stained lipid clusters. **(I):** Alizarin red staining of GFP-DPSC cultured in osteogenic medium (magnification, ×100). Scale bars = 100 μm **(B, E)**, 10 μm **([D]**, left panel), 0.5 μm **([D]**, right panel), and 25 μm **(H)**. Abbreviations: CPD, cumulative population doublings; FSC, forward scatter; GFP, green fluorescent protein; P, passage.

Table 1. Echocardiographic values of saline and DPSC groups

	Saline (n = 9)					DPSC (n = 7)				
Parameters	Baseline	MI	2 w	4 w	p, MI vs. 4 w	Baseline	MI	2 w	4 w	p, MI vs. 4 w
AWd (mm)	1.17 ± 0.07	0.93 ± 0.06	0.91 ± 0.06	1.09 ± 0.05	NS	1.23 ± 0.09	0.81 ± 0.08	1.20 ± 0.08	1.11 ± 0.07	<.03
LVd (mm)	5.81 ± 0.22	6.53 ± 0.15	7.16 ± 0.19	7.60 ± 0.18	<.02	5.65 ± 0.22	6.74 ± 0.21	7.01 ± 0.26	7.26 ± 0.32	NS
PWd (mm)	1.29 ± 0.05	1.41 ± 0.11	1.34 ± 0.07	1.31 ± 0.07	NS	1.29 ± 0.14	1.07 ± 0.05	1.34 ± 0.13	1.31 ± 0.10	<.03
AWs (mm)	2.20 ± 0.11	1.37 ± 0.16	1.38 ± 0.11	1.49 ± 0.10	NS	2.35 ± 0.17	1.24 ± 0.11	1.98 ± 0.08	1.94 ± 0.10	<.03
LVs (mm)	3.12 ± 0.20	4.76 ± 1.34	5.27 ± 0.22	5.63 ± 0.23	<.05	3.33 ± 0.09	4.74 ± 0.24	4.63 ± 0.30	4.94 ± 0.24	NS
PWs (mm)	2.08 ± 0.14	2.15 ± 0.11	2.06 ± 0.10	1.93 ± 0.10	NS	2.10 ± 0.13	1.83 ± 0.12	2.09 ± 0.07	2.10 ± 0.12	NS
EDA (mm^2)	29.0 ± 1.2	34.3 ± 2.3	39.9 ± 1.7	42.4 ± 1.5	<.02	27.8 ± 0.7	40.0 ± 2.7	44.9 ± 3.0	45.1 ± 2.1	NS
ESA (mm^2)	7.7 ± 0.5	19.6 ± 1.5	22.8 ± 1.6	24.9 ± 2.0	<.03	7.0 ± 0.4	23.1 ± 2.7	21.3 ± 2.9	19.9 ± 0.2	NS
FS (%)	46.6 ± 2.0	26.6 ± 1.6	26.3 ± 1.9	24.2 ± 1.6	NS	40.8 ± 1.1	28.8 ± 2.1	31.2 ± 1.7	32.9 ± 1.6	NS
FAC (%)	77.4 ± 1.0	41.1 ± 2.2	40.9 ± 2.3	38.4 ± 2.8	NS	74.9 ± 0.8	42.9 ± 2.9	53.6 ± 3.7	55.8 ± 1.4	<.02
AWT (%)	93.2 ± 10.1	45.8 ± 5.3	41.7 ± 7.1	31.7 ± 5.1	NS	92.7 ± 10.8	50.0 ± 10.0	62.5 ± 4.7	78.3 ± 10.1	<.05

All values are mean ± SEM. Three DPSC samples were used.
Abbreviations: AWd, anterior wall diastole thickness; AWs, anterior wall systole thickness; AWT, anterior wall thickening; DPSC, dental pulp stem cells; EDA, end-diastolic area; ESA, end-systolic area; FAC, fractional area change; FS, fractional shortening; LVd, left ventricular diastole internal dimension; LVs, left ventricular systole internal dimension; MI, myocardial infarction; NS, not significant; PWd, posterior wall diastole thickness; PWs, posterior wall systole thickness; w, weeks.

equal volume of saline) in five injections of a 5-μl volume at five points of the infarct border zone with a Hamilton syringe.

Functional Assessment by Echocardiography

Rats were anesthetized with inhalatory anesthesia (Sevorane), the chest was shaved, and the rats were placed in the supine position. Transthoracic echocardiography was performed by a blinded echocardiographist using a General Electric system (Vivid 7; GE Healthcare, Little Chalfont, U.K., http://www.gehealthcare.com) equipped with a 10-MHz linear-array transducer. Measurements were taken at baseline (1 day preinfarction), postinfarction (7 days), and post-transplantation (2 and 4 weeks). M-Mode and two-dimensional (2D) echocardiography was performed at the level of the papillary muscles in the parasternal short axis view. Functional parameters over five consecutive cardiac cycles were calculated using standard methods [27]. Left ventricular (LV) internal dimensions at end diastole (LVd) and end systole (LVs), anterior wall (AW) dimensions, and posterior wall (PW) dimensions in diastole and systole were quantified in M-Mode. End-diastolic area (EDA) and end-systolic area (ESA) were quantified in 2D images. Percentage changes in AW and PW thickening were calculated as percentage of anterior wall thickening (AWT) = (AWs/AWd − 1) × 100 and percentage of PW thickening = (PWs/PWd − 1) × 100, respectively, where AWs is anterior wall systole thickness, AWd is anterior wall diastole thickness, PWs is posterior wall systole thickness, and PWd is posterior wall diastole thickness. Fractional shortening was calculated as [(LVDd − LVDs)/LVDd] × 100. Fractional area change (FAC) was calculated as percentage of FAC = [(EDA − ESA)/EDA] × 100.

Immunohistochemistry and Electron Microscopy

At 4 weeks postimplantation, animals were euthanized with an overdose of ketamine (125 mg/kg), valium (10 mg/kg), and atropine (50 mg/kg), and the hearts were removed, washed with phosphate-buffered saline, and fixed in 2% paraformaldehyde (PFA) or 2% PFA/glutaraldehyde for electron microscopy examination. The hearts were cryopreserved with 20% sucrose, embedded in Tissue-Tek OCT Compound (Sakura Finetek, Torrance, CA, http://www.sakura.com), and cut into 14-μm slices. To assess the differentiation of human cells, serial sections were stained with antibodies against CD90 (Becton Dickinson), cardiac troponin (cTnI) (Santa Cruz Biotechnology Inc., Santa Cruz, CA, http://www.scbt.com), β-myosin heavy chain (β-MHC) (Chemicon, Temecula, CA, http://www.chemicon.com), smooth muscle actin (SMA) (Sigma-Aldrich, St. Louis, http://www.sigmaaldrich.com), Myo D (Chemicon), human nuclei antibody (Chemicon), and Ki67 (Novocastra Ltd., Newcastle upon Tyne,

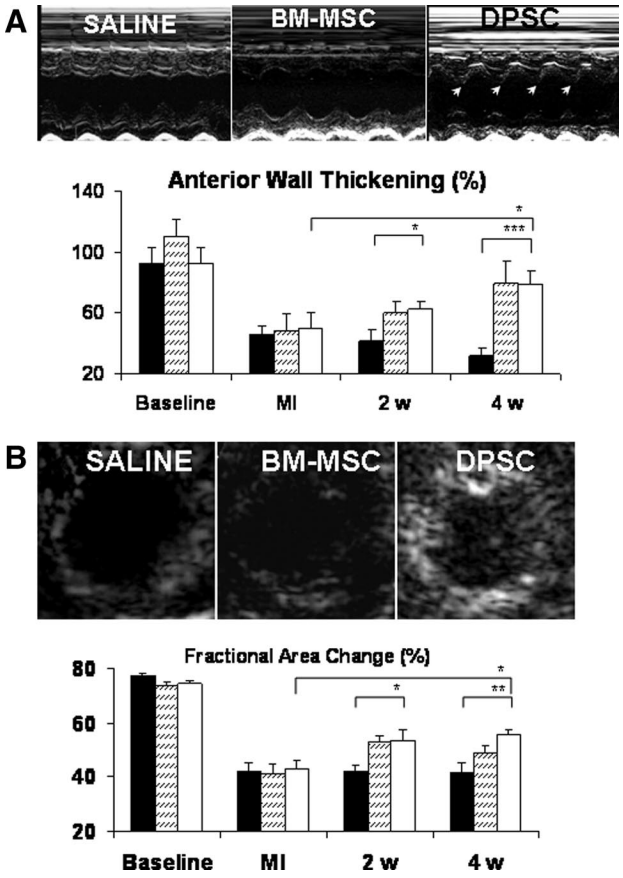

Figure 2. Improvement of left ventricular function in DPSC-treated animals. **(A):** Representative echocardiographic images of one animal from saline, BM-MSC, and DPSC groups in M-Mode imaging are shown. Quantified values of anterior wall thickening (%) are given. **(B):** A representative two-dimensional systolic frame echocardiograph showing differences in wall motion is shown. Values of fractional area change (%) are given. Data are expressed as mean ± SEM and correspond to n = 9 animals (saline), n = 7 animals (BM-MSC), and n = 7 animals (DPSC). Columns represent the saline group (solid columns), BM-MSC group (striped columns), and DPSC group (open columns). *, $p < .05$; **, $p < .01$; ***, $p < .001$. Abbreviations: BM-MSC, bone marrow mesenchymal stem cell; DPSC, dental pulp stem cells; MI, myocardial infarction; w, weeks.

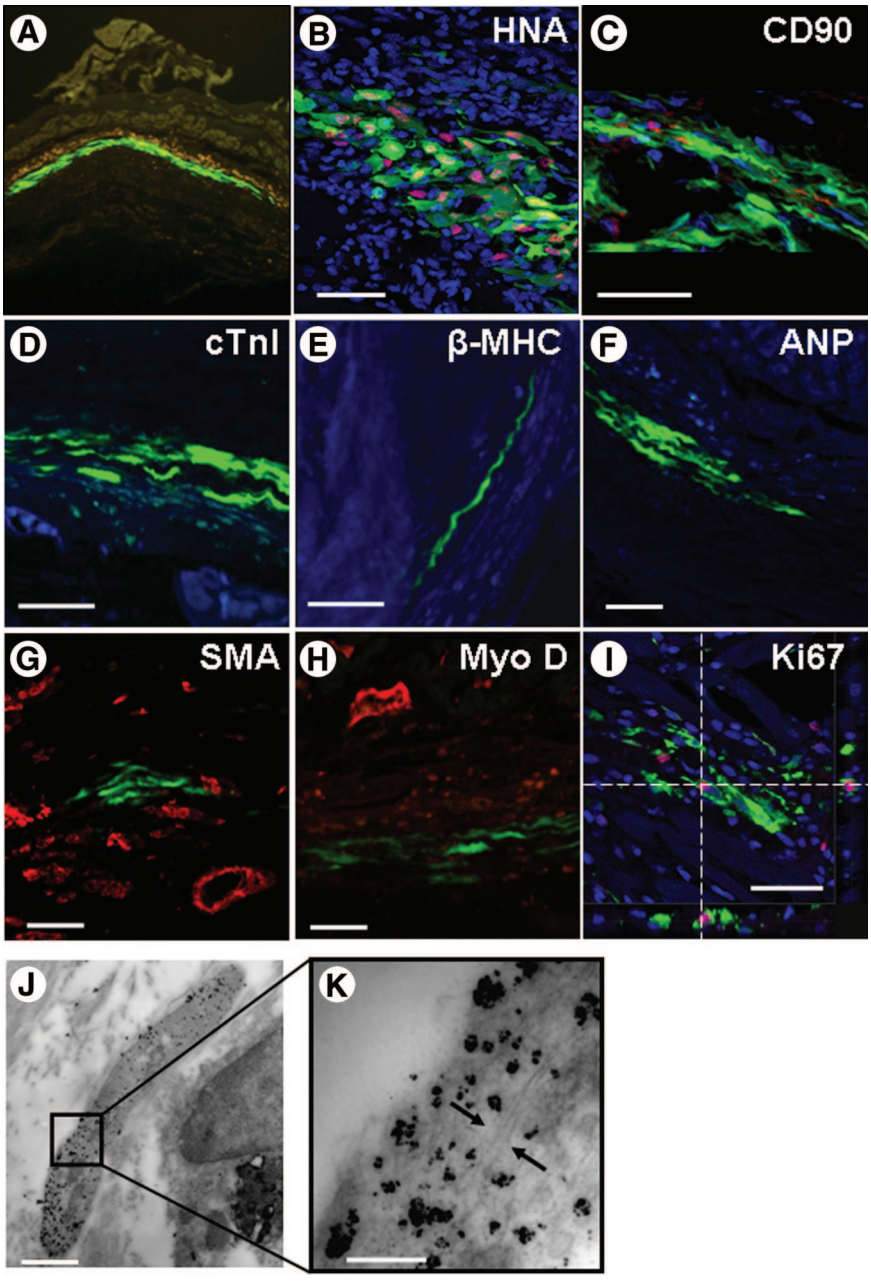

Figure 3. Engraftment of dental pulp stem cells (DPSC) in infarcted heart showing lack of in vivo differentiation of DPSC to cardiac or smooth muscle cells at 4 weeks post-transplantation. **(A):** Green fluorescent protein (GFP)-DPSC (green epifluorescence) graft in the ischemic myocardial tissue. **(B):** Reactivity of GFP-DPSC with HNA. **(C):** Positive staining of GFP-DPSC engrafted in heart tissue with anti-human CD90 antibody. **(D–H):** Immunohistochemistry of tissue sections showing the negative staining of GFP-DPSC with antibodies against cTnI (blue), β-MHC (blue), ANP (blue), SMA (red), and Myo D (red). **(I):** Ki67 staining of engrafted GFP-DPSC. Photomicrographs in **(B–I)** were obtained using confocal microscopy and are representative of experiments from three GFP-DPSC samples. **(J):** Left ventricle wall ultrathin section showing a colloidal gold-labeled GFP-DPSC. **(K):** Detailed ultrastructure of the cell shown in G. Arrows point a filament bundle. Scale bars = 50 μm **(B–I)**, 1 μm **(J)**, and 0.4 μm **(K)**. Abbreviations: ANP, atrial natriuretic peptide; cTnI, cardiac troponin; HNA, human nuclei antibody; β-MHC, β-myosin heavy chain; SMA, smooth muscle actin.

U.K., http://www.novocastra.co.uk). Goat anti-rabbit secondary antibodies were coupled to rhodamine (Jackson Immunoresearch Laboratories, West Grove, PA, http://www.jacksonimmuno.com) or Cascade Blue (Molecular Probes, Eugene, OR, http://probes.invitrogen.com). Tissue samples were analyzed by confocal microscopy (TCS-SP2-AOB5; Leica, Heerbrugg, Switzerland, http://www.leica.com). Immunogold staining was performed on cryopreserved slices (50 μm) with anti-GFP chicken antibody (Aves Labs, Tigard, OR, http://www.aveslab.com) followed by a colloidal secondary antibody (Electron Microscopy Sciences, Hatfield, PA, http://www.emsdiasum.com).

For electron microscopy studies, transverse sections of 50 μm were cut on a cryostat. The sections were postfixed in 2% osmium for 2 hours, rinsed, rehydrated, and embedded in Araldite (Durcupan; Fluka Biochemica, Rokokoma, NY, http://www.sigmaaldrich.com). Serial 1.5-μm semithin sections were cut with a diamond knife and stained with 1% toluidine blue. For identification of individual cells ultrathin (0.05 μm) sections were cut with a diamond knife, stained with lead citrate, and examined under an FEI Tecnai spirit electron microscope (Hillsboro, OR, http://www.feicompany.com).

Vascular Density and Immunohistochemical Analysis

To detect newly formed vessels, rats from each group were euthanized at 4 weeks post-transplantation and examined via immunohistochemistry for expression of CD31 (Chemicon). Vessels were counted in 10 fields in the peri-infarct zone at a magnification of $\times$200. The number of vessels per unit area (mm^2) was determined using Image Pro Plus (version 5.1) to evaluate light micrographs.

Morphometry

The LV infarct size was measured in 8–12 transverse sections of 14 μm (one slice every 200 μm of tissue from apex to base) stained with Masson's trichrome. The fibrotic zone was identified by the light blue color; scar area was determined by computer planimetry of the fibrotic regions using Image Pro Plus (version 5.1) software.

All studies were performed in a blinded fashion. Infarct size was expressed as percentage of total left ventricular area and as a mean of all slices from each heart.

Statistical Analysis

Data are expressed as mean ± SEM. Comparisons between MI and 4 weeks post-transplantation were performed with a paired Student *t* test. Comparisons of control and experimental groups were done with the Wilcoxon test. Statistical values were calculated using the SPSS software (SPSS, Chicago, http://www.spss.com). Differences were considered statistically significant at $p < .05$ with a 95% confidence interval.

RESULTS

Characterization and Retroviral Infection of Expanded Human DPSC

Dental pulp isolated from the pulp chamber (Fig. 1A) was digested, and cells were seeded in growth medium. At 1 week, adherent cells were detected (Fig. 1B). Two weeks after plating, the adherent cells, covering 80% of the surface, were detached and seeded for further expansion and retroviral infection (for labeling with eGFP). As assessed by flow cytometry, DPSC constituted a homogeneous population, positive for CD29, CD44, CD90, CD105, and CD166; slightly positive for CD117 (Fig. 1C); and negative for CD14, CD34, CD45, CD106, and VEGFR-2 (not shown), indicating an MSC-like phenotype. Ultrastructural analysis showed lax chromatin, numerous cytoplasmic organules, rough endoplasmic reticulum, small Golgi apparatus, and filaments distributed along the cytoplasm (Fig. 1D, arrows). When DPSC were GFP-transduced, more than 50% of cells were labeled (Fig. 1E); after three to four rounds of infection, ~99% of cultured cells were GFP-positive (Fig. 1F). Retroviral infection did not affect either their proliferation capacity (Fig. 1G), the ability to transdifferentiate into adipocytes (Fig. 1H) and osteocytes (Fig. 1I), or the surface antigen expression of DPSC as assessed by flow cytometry (passages 5–10; not shown).

DPSC Transplantation Improves Cardiac Function After Myocardial Infarction

The echocardiographic parameters from saline and DPSC groups are listed in Table 1. At baseline and after MI, the values of the echocardiographic parameters analyzed were similar in treated and untreated animals, indicating comparable levels of tissue injury. In the saline group, there was a progressive significant deterioration of cardiac systolic function measured in terms of LV internal dimension (systole and diastole), EDA, and ESA (Table 1).

DPSC treatment resulted in an improvement of all parameters measured 4 weeks post-transplantation versus MI values, whereas these changes were not appreciated in the saline group. The DPSC group showed an improvement in systolic function calculated in FAC (%): 42.9 ± 2.9 versus 55.8 ± 1.4; $p < .02$. In this group, there was also a significant increase in AWT (%), changing from 50.0 ± 10.0 after MI to 78.3 ± 10.1, 4 weeks after DPSC transplantation ($p < .05$). Wilcoxon test showed significant differences between saline and DPSC groups as soon as 2 weeks post-transplantation in the AWT (%), and FAC (%) parameters (Fig. 2A, 2B), which persisted along the time studied (4 weeks). To compare the effects of DPSC with those induced by the more extensively studied BM-MSC, a new group of animals transplanted with BM-MSC was included in the study as positive control (Fig. 2A, 2B). The degree of improvement was similar in both experimental groups (AWT [%]: 78.3 ± 10.1 in DPSC group vs. 79.3 ± 15.0 in BM-MSC group; FAC [%]: 55.8 ± 1.4 vs. 48.90 ± 2.69, without significant differences in all the parameters measured [not shown]). Video recording of cardiac motility showed an improvement in contractility in the DPSC group but not in the saline group (supplemental online data).

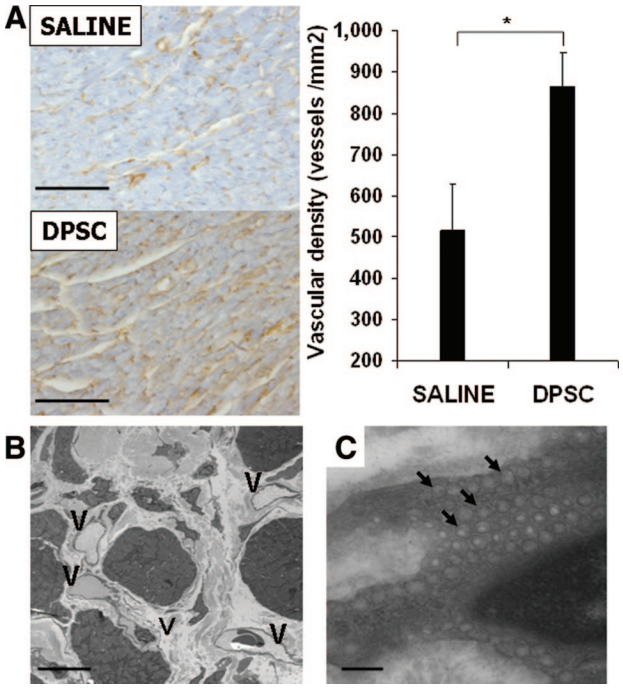

Figure 4. Neovascularization in the infarct area 4 weeks after cell transplantation. **(A):** A representative section of control and DPSC-treated animals stained with anti-CD31, and quantification of the total number of V in both groups ($n = 8$; ∗, $p < .05$). **(B):** Ultrastructural analysis of the peri-infarct zone from a DPSC-transplanted animal showing V surrounding cardiomyocyte area. **(C):** Detail of a cell from a wall V showing multiple caveolae. Scale bars = 100 μm **(A)**, 10 μm **(B)**, and 0.2 μm **(C)**. Abbreviations: DPSC, dental pulp stem cells; V, vessels.

DPSC Do Not Differentiate into Cardiac or Smooth Muscle Cells

Analysis of cell engraftment was followed by the green epifluorescence of eGFP-DPSC. Human green cells were often located in the infarcted regions of tissue (Fig. 3A). To assess whether DPSC maintained their original phenotypic pattern in vivo or they differentiate into cardiac or smooth muscle cells, cryopreserved heart tissue sections were analyzed by immunohistochemistry under the confocal microscope. One month after transplantation, engrafted GFP cells were all of human origin, as detected by human nuclei antibody (Fig. 3B), and approximately 50% of engrafted cells still maintained the CD90 expression (Fig. 3C). However, none of the human GFP cells detected were labeled with antibodies against cTnI (Fig. 3D), atrial natriuretic peptide (Fig. 3E), β-MHC (Fig. 3F), SMA (Fig. 3G), or Myo D (Fig. 3H), indicating that the transplanted cells did not differentiate into cardiac or smooth muscle cells. In addition, we did not find expression of endothelial markers or association of DPSC with the vascular network (data not shown). Engrafted DPSC maintained their ability to proliferate, as some GFP-DPSC positive for Ki67 staining were observed (Fig. 3I). To further investigate DPSC differentiation, we performed immunogold staining followed by electron microscopy. DPSC were localized in the granulated tissue but not in the cardiomyocyte bundles (Fig. 3J). Gold-labeled cells showed ultrastructure similar to that observed in

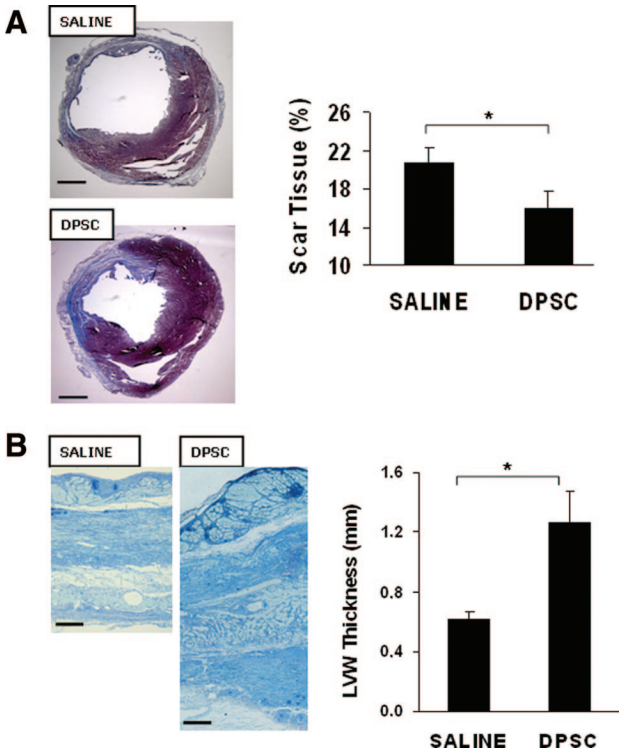

Figure 5. Effect of DPSC transplantation on infarct size. **(A):** Representative heart sections from infarcted nude rats receiving saline or DPSC. Fibrotic area in the left ventricle was calculated in Masson's trichrome-stained sections. **(B):** Semithin sections and quantification of the LVW thickness. Animals were euthanized 4 weeks post-transplantation. Values are the mean ± SEM corresponding to $n = 9$ and $n = 8$ for control and DPSC groups, respectively. *, $p < .05$. Abbreviations: DPSC, dental pulp stem cells; LVW, left ventricular wall.

vitro (Fig. 1D), with typical filaments along the cytoplasm (Fig. 3K, arrows) and the absence of sarcomeres, Z-line regions, or other cardiomyocyte-like structures, corroborating the lack of DPSC differentiation into cardiac cells.

Angiogenesis Induced by MSC

Vascular density was evaluated in the LV wall 30 days postimplantation by immunostaining with anti-CD31 antibody. The total number of vessels was significantly higher in the DPSC group than in the saline group (865.2 ± 82.0 vs. 515.0 ± 113.8; $p < .05$) (Fig. 4A). These vessels were of rat origin; they contained blood cells, indicating their functionality (Fig. 4B); and they showed multiple caveolae, as analyzed by electron microscopy (Fig. 4C) (the presence of multiple caveolae is related to the dynamic state of vascular cells).

DPSC Transplantation Reduces Infarcted Area

Cross-sections from DPSC and control animals were stained with Masson's trichrome and used to quantify the infarcted area in each animal. The area of fibrous scar tissue referred to as the total LV area was smaller in DPSC transplanted animals than in saline controls (15.9% ± 1.7% vs. 21.2% ± 1.6%; $p < .05$) (Fig. 5A). Moreover, semithin sections of LV walls showed a significant increase in DPSC-treated animals (0.62 ± 0.05 mm in control group vs. 1.26 ± 0.21 mm in DPSC group; $p < .05$) (Fig. 5B).

Organization of the Infarcted Tissue

To further investigate the morphological changes induced by DPSC transplantation, we obtained ultrathin sections of cardiac tissue from four animals of each group and analyzed the differences by electron microscopy. As can be seen in Figure 6, analysis of ultrathin sections revealed bands of myocardial tissue disposed between the fibrotic layers only in the DPSC group; these bands were accompanied by an increase in the number of capillaries, as had been previously observed with the assays mentioned above. In addition, this higher resolution allowed us to visualize that cardiomyocyte bundles were healthy in the DPSC sections, probably because of the great number of vessels surrounding them, whereas they showed a notable degree of necrosis in control animals (not shown).

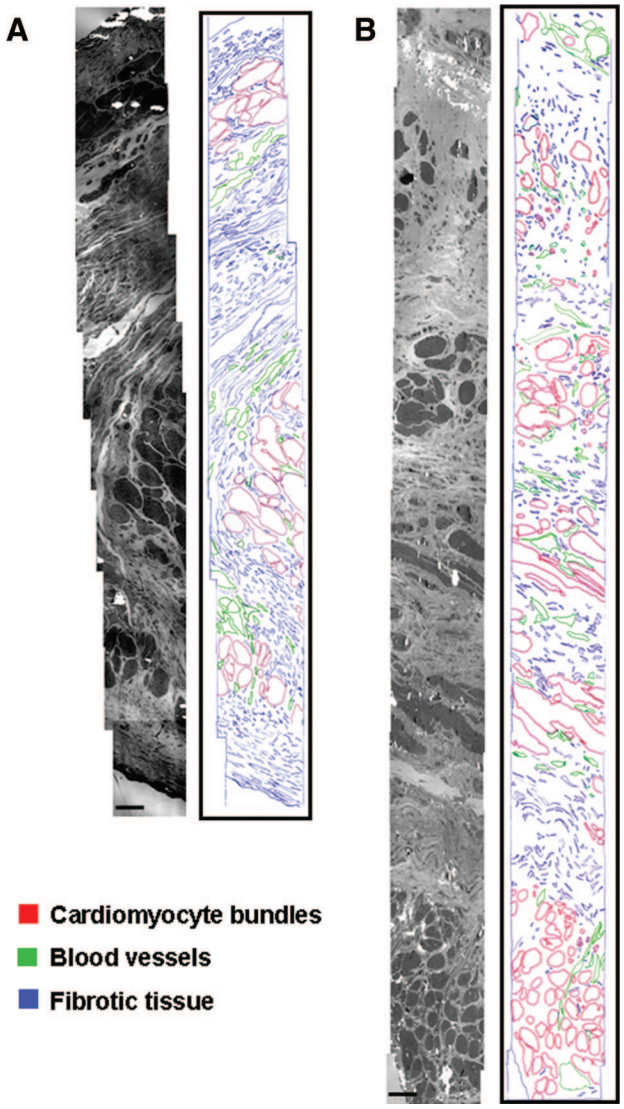

Figure 6. Organization of cardiac tissue in the peri-infarct zone. **(A, B):** Representative ultrathin sections of left ventricular walls at the peri-infarct zone from a control animal and a dental pulp stem cell-treated animal, respectively. Contiguous electron micrographs were assembled into a photomontage. The contours of the different cell types were traced in different colors. Scale bars = 5 μm.

DISCUSSION

We demonstrate that DPSC constitute an alternative to BM-MSC in the armamentarium for cardiac repair. As true MSC, DPSC can survive and engraft in ischemic environments. The

degree of restoration of cardiac function with DPSC transplantation was comparable to that observed with BM-MSC, and no significant differences were found between both groups. The improvement was especially noticeable in the percentage of AWT and FAC, indicating that DPSC transplantation not only prevents ventricular remodeling but also improves the regional contractility. Indeed, improvement in cardiac function was correlated with reduction of infarct size, higher capillary density, and increased wall thickness in DPSC-transplanted animals. In addition, ultrastructural analysis of LV wall peri-infarct zones showed an increase in cardiomyocyte bundles that reduced infarcted area and a higher proportion of myofibroblasts in the DPSC group (not shown). Myofibroblasts have been associated with the wound healing that occurs after ischemia, and their ontogenesis is related to the morphological changes observed in the fibroblasts when they are subjected to stress tension [28, 29]. Moreover, the onset of angiogenesis was closely correlated with repopulation of infarcted area with myofibroblasts in a mouse model of cardiomyopathy [30]. Thus, myofibroblasts could also account for the recovery of the LV tissue in DPSC group.

DPSC induced cardiac repair in the absence of cell differentiation. Although no specific experiments were performed to explore differentiation versus fusion, both phenomena were excluded since no expression of cardiac or smooth muscle markers was observed by confocal or electron microscopy analysis in GFP-transplanted cells. These results are in accordance with previous reports that support the ability of MSC to induce cardiac repair despite extremely rare fusion/differentiation events [10, 31–35]. However, we cannot rule out the possibility that longer periods of transplantation are necessary to induce the expression of cardiac markers in these cells, since allogeneic BM-MSC transplanted in the ischemic myocardium required between 3 and 6 months to express muscle markers [10].

The data presented here suggest that the benefits observed after DPSC transplantation could be due to secretion of paracrine factors. In this context, adipose tissue-derived MSC, transplanted as a monolayer, increased wall thickness and improved cardiac function after myocardial infarction through secretion of hepatocyte growth factor and VEGF [31]. Moreover, using the c-kit mutant $Kit^{W}/Kit^{W\text{-}v}$ mice, it has been demonstrated that BM-derived c-kit^{+} cells improved cardiac function by increasing VEGF and reversing the cardiac ratio of angiopoietin-1 to angiopoietin-2 [30, 36]. Regarding the possible factors involved in DPSC-mediated repair, one may speculate that VEGF could be one such factor, since secretion of VEGF in physiological amounts by DPSC is able to induce the formation of capillary-like networks in an ex vivo model of angiogenesis [18]. Considering that human DPSC have a level of gene expression similar to that of BM-MSC [13, 37], it is also possible that other cytokines, such as IGF and SCF, secreted by DPSC could also contribute to the cardiac regeneration and improvement of LV function. Supporting this is the observation that these two cytokines show a cardioprotective effect when administered after MI [23, 38]. However, additional experiments should be performed to determine the possible factors responsible for this recovery.

Conclusion

DPSC are able to repair infarcted myocardium, and this is associated with an increase in the number of vessels and a reduction in infarct size, probably because of their ability to secrete proangiogenic and antiapoptotic factors. The degree of cardiac repair observed is similar to that obtained with BM-MSC. Therefore, this study extends the knowledge of DPSC therapeutical properties and provides a new source of stem cells for the treatment of ischemic diseases.

Acknowledgments

This work was supported by grants from the Instituto de Salud Carlos III for the Regenerative Medicine Program of Valencian Community to Centro de Investigación Principe Felipe and from the Fondo de Investigaciones Sanitarias (PI04/2366, PI03/136). P.S. is the recipient of a contract from the Instituto de Salud Carlos III. A.A. is a predoctoral fellow from the Centro de Investigación Principe Felipe. We are indebted to Dr. A Chapel for the gift of the PG13-PSF-GFP cell line. We thank J. Farré for technical assistance in flow cytometry experiments, Dr. J. Barea for collecting the third molar samples, and Dr. D. Taylor for comments and advice in the elaboration of the manuscript. C.G. and A.A. contributed equally to this work.

Disclosure of Potential Conflicts of Interest

The authors indicate no potential conflicts of interest.

References

1 Zuk PA, Zhu M, Ashjian P et al. Human adipose tissue is a source of multipotent stem cells. Mol Biol Cell 2002;13:4279–4295.
2 Young HE, Steele TA, Bray RA et al. Human reserve pluripotent mesenchymal stem cells are present in the connective tissues of skeletal muscle and dermis derived from fetal, adult, and geriatric donors. Anat Rec 2001;264:51–62.
3 Su EJ, Cioffi CL, Stefansson S et al. Gene therapy vector-mediated expression of insulin-like growth factors protects cardiomyocytes from apoptosis and enhances neovascularization. Am J Physiol Heart Circ Physiol 2003;284:H1429–H1440.
4 Romanov YA, Svintsitskaya VA, Smirnov VN. Searching for alternative sources of postnatal human mesenchymal stem cells: Candidate MSC-like cells from umbilical cord. STEM CELLS 2003;21:105–110.
5 Yen BL, Huang HI, Chien CC et al. Isolation of multipotent cells from human term placenta. STEM CELLS 2005;23:3–9.
6 Gronthos SMM, Brahim J, Robey PG et al. Postnatal human dental pulp stem cells (DPSCs) in vitro and in vivo. Proc Natl Acad Sci U S A 2000;97:13625–13630.
7 Kern S, Eichler H, Stoeve J et al. Comparative analysis of mesenchymal stem cells from bone marrow, umbilical cord blood, or adipose tissue. STEM CELLS 2006;24:1294–1301.
8 Liechty KW, MacKenzie TC, Shaaban AF et al. Human mesenchymal stem cells engraft and demonstrate site-specific differentiation after in utero transplantation in sheep. Nat Med 2000;6:1282–1286.
9 Davani S, Marandin A, Mersin N et al. Mesenchymal progenitor cells differentiate into an endothelial phenotype, enhance vascular density, and improve heart function in a rat cellular cardiomyoplasty model. Circulation 2003;108(suppl 1):II253–II258.
10 Dai W, Hale SL, Martin BJ et al. Allogeneic mesenchymal stem cell transplantation in postinfarcted rat myocardium: Short- and long-term effects. Circulation 2005;112:214–223.
11 Nagaya N, Kangawa K, Itoh T et al. Transplantation of mesenchymal stem cells improves cardiac function in a rat model of dilated cardiomyopathy. Circulation 2005;112:1128–1135.
12 Wang JS, Shum-Tim D, Galipeau J et al. Marrow stromal cells for cellular cardiomyoplasty: Feasibility and potential clinical advantages. J Thorac Cardiovasc Surg 2000;120:999–1005.
13 Shi S, Robey PG, Gronthos S. Comparison of human dental pulp and bone marrow stromal stem cells by cDNA microarray analysis. Bone 2001;29:532–539.
14 Yamada Y, Fujimoto A, Ito A et al. Cluster analysis and gene expression profiles: A cDNA microarray system-based comparison between human dental pulp stem cells (hDPSCs) and human mesenchymal stem cells

(hMSCs) for tissue engineering cell therapy. Biomaterials 2006;27: 3766–3781.
15 Pierdomenico L, Bonsi L, Calvitti M et al. Multipotent mesenchymal stem cells with immunosuppressive activity can be easily isolated from dental pulp. Transplantation 2005;80:836–842.
16 Matsushita K, Motani R, Sakuta T et al. The role of vascular endothelial growth factor in human dental pulp cells: Induction of chemotaxis, proliferation, and differentiation and activation of the AP-1-dependent signaling pathway. J Dent Res 2000;79:1596–1603.
17 Artese L, Rubini C, Ferrero G et al. Vascular endothelial growth factor (VEGF) expression in healthy and inflamed human dental pulps. J Endod 2002;28:20–23.
18 Tran-Hung L, Mathieu S, About I. Role of human pulp fibroblasts in angiogenesis. J Dent Res 2006;85:819–823.
19 Caviedes-Bucheli J, Munoz HR, Rodriguez CE et al. Expression of insulin-like growth factor-1 receptor in human pulp tissue. J Endod 2004;30:767–769.
20 Reichenmiller KM, Mattern C, Ranke MB et al. IGFs, IGFBPs, IGF-binding sites and biochemical markers of bone metabolism during differentiation in human pulp fibroblasts. Horm Res 2004;62:33–39.
21 Sawa Y, Horie Y, Yamaoka Y et al. Production of colony-stimulating factor in human dental pulp fibroblasts. J Dent Res 2003;82:96–100.
22 Gagari E, Rand MK, Tayari L et al. Expression of stem cell factor and its receptor, c-kit, in human oral mesenchymal cells. Eur J Oral Sci 2006; 114:409–415.
23 Duerr RL, Huang S, Miraliakbar HR et al. Insulin-like growth factor-1 enhances ventricular hypertrophy and function during the onset of experimental cardiac failure. J Clin Invest 1995;95:619–627.
24 Aikawa R, Nawano M, Gu Y et al. Insulin prevents cardiomyocytes from oxidative stress-induced apoptosis through activation of PI3 kinase/Akt. Circulation 2000;102:2873–2879.
25 Friedrich J, Apstein CS, Ingwall JS. 31P nuclear magnetic resonance spectroscopic imaging of regions of remodeled myocardium in the infarcted rat heart. Circulation 1995;92:3527–3538.
26 Agbulut O, Vandervelde S, Al Attar N et al. Comparison of human skeletal myoblasts and bone marrow-derived CD133+ progenitors for the repair of infarcted myocardium. J Am Coll Cardiol 2004;44: 458–463.
27 Litwin SE, Katz SE, Morgan JP et al. Serial echocardiographic assessment of left ventricular geometry and function after large myocardial infarction in the rat. Circulation 1994;89:345–354.
28 Tomasek JJ, Gabbiani G, Hinz B et al. Myofibroblasts and mechano-regulation of connective tissue remodelling. Nat Rev Mol Cell Biol 2002;3:349–363.
29 Wang J, Chen H, Seth A et al. Mechanical force regulation of myofibroblast differentiation in cardiac fibroblasts. Am J Physiol Heart Circ Physiol 2003;285:H1871–H1881.
30 Fazel S, Cimini M, Chen L et al. Cardioprotective c-kit+ cells are from the bone marrow and regulate the myocardial balance of angiogenic cytokines. J Clin Invest 2006;116:1865–1877.
31 Miyahara YNN, Kataoka M, Yanagawa B et al. Monolayered mesenchymal stem cells repair scarred myocardium after myocardial infarction. Nat Med 2006;12:459–465.
32 Mangi AA, Noiseux N, Kong D et al. Mesenchymal stem cells modified with Akt prevent remodeling and restore performance of infarcted hearts. Nat Med 2003;9:1195–1201.
33 Noiseux N, Gnecchi M, Lopez-Ilasaca M et al. Mesenchymal stem cells overexpressing Akt dramatically repair infarcted myocardium and improve cardiac function despite infrequent cellular fusion or differentiation. Mol Ther 2006;14:840–850.
34 Gnecchi M, He H, Noiseux N et al. Evidence supporting paracrine hypothesis for Akt-modified mesenchymal stem cell-mediated cardiac protection and functional improvement. FASEB J 2006;20:661–669.
35 Uemura R, Xu M, Ahmad N et al. Bone marrow stem cells prevent left ventricular remodeling of ischemic heart through paracrine signaling. Circ Res 2006;98:1414–1421.
36 Chien KR. Lost and found: Cardiac stem cell therapy revisited. J Clin Invest 2006;116:1838–1840.
37 Kinnaird T, Stabile E, Burnett MS et al. Marrow-derived stromal cells express genes encoding a broad spectrum of arteriogenic cytokines and promote in vitro and in vivo arteriogenesis through paracrine mechanisms. Circ Res 2004;94:678–685.
38 Dawn B, Guo Y, Rezazadeh A et al. Postinfarct cytokine therapy regenerates cardiac tissue and improves left ventricular function. Circ Res 2006;98:1098–1105.


See www.StemCells.com for supplemental material available online.

Human Dental Pulp Stem Cells Improve Left Ventricular Function, Induce Angiogenesis, and Reduce Infarct Size in Rats with Acute Myocardial Infarction

Carolina Gandia, Ana Armiñan, Jose Manuel García-Verdugo, Elisa Lledó, Amparo Ruiz, M Dolores Miñana, Jorge Sanchez-Torrijos, Rafael Payá, Vicente Mirabet, Francisco Carbonell-Uberos, Mauro Llop, Jose Anastasio Montero and Pilar Sepúlveda

Stem Cells 2008;26;638-645; originally published online Dec 13, 2007;
DOI: 10.1634/stemcells.2007-0484